J. Membrane Biol. 65, 185-196 (1982)

The Journal of
Membrane Biology

Electrical Properties of Chloride Transport across the *Necturus* Proximal Tubule

William B. Guggino, Emile L. Boulpaep, and Gerhard Giebisch

Department of Physiology, Yale University School of Medicine, New Haven, Connecticut 06510

Summary. The chloride conductance of the basolateral cell membrane of the *Necturus* proximal tubule was studied using conventional and chloride-sensitive liquid ion exchange microelectrodes. Individual apical and basolateral cell membrane and shunt resistances, transepithelial and basolateral cell membrane potential differences, and electromotive forces were determined in control and after reductions in extracellular Cl^-. When extracellular Cl^- activity is reduced in both apical and basolateral solutions the resistance of the shunt increases about 2.8 times over control without any significant change in cell membrane resistances. This suggests a high Cl^- conductance of the paracellular shunt but a low Cl^- conductance of the cell membranes. Reduction of Cl^- in both bathing solutions or only on the basolateral side hyperpolarizes both the basolateral cell membrane potential difference and electromotive force. Hyperpolarization of the basolateral cell membrane potential difference after low Cl^- perfusion was abolished by exposure to HCO_3^--free solutions and SITS treatment. In control conditions, intracellular Cl^- activity was significantly higher than predicted from the equilibrium distribution across both the apical and basolateral cell membranes. Reducing Cl^- in only the basolateral solution caused a decrease in intracellular Cl^-. From an estimate of the net Cl^- flux across the basolateral cell membrane and the electrochemical driving force, a Cl^- conductance of the basolateral cell membrane was predicted and compared to measured values. It was concluded that the Cl^- conductance of the basolateral cell membrane was not large enough to account for the measured flux of Cl^- by electrodiffusion alone. Therefore these results suggest the presence of an electroneutral mechanism for Cl^- transport across the basolateral cell membrane of the *Necturus* proximal tubule cell.

Key words proximal tubule · chloride transport · membrane resistance · intracellular chloride activity

Introduction

Chloride enters the cells of a wide variety of NaCl absorbing epithelia across the apical cell membranes by means of electroneutral, coupled sodium and chloride transport [15]. These epithelia transport chloride across the apical cell membrane against an electrochemical gradient, the energy for the uphill movement of Cl^- being derived from the downhill chemical gradient for Na^+ across the apical cell membrane. The Na^+ gradient across the luminal cell membrane is established by the active transport of sodium across the basolateral cell membrane via the Na/K pump.

A common feature of these epithelia is that intracellular Cl^- activity is higher than predicted from the electrical potential difference across the apical membrane. For example, the measured intracellular Cl^- activity exceeds the activity predicted from the passive chloride distribution across the apical cell membrane by a factor of 2.4 in the rabbit gallbladder [13], 2.3 in the bullfrog small intestine [6], and 3.4 in the winter flounder small intestine [12].

The intracellular chloride activity of the *Necturus* proximal tubule cell has also been shown to be above the value predicted for passive distribution [21, 26]. Spring and Kimura [26] found that the entry of chloride into the cell across the apical cell membrane requires the presence of sodium in the tubular lumen and that intracellular chloride activity is independent of variations of the electrical potential difference. They postulated that chloride enters the cell across the apical membrane via a saturable, electroneutral, carrier-mediated mechanism involving coupled sodium and chloride transport.

Because intracellular chloride activity is above equilibrium in those epithelial cells that exhibit apical NaCl cotransport, there is a favorable electrochemical gradient for chloride exit across the basolateral cell membrane. Therefore, it is possible that chloride transport across the basolateral cell membrane could be completely electrodiffusive provided there is an adequately large basolateral chloride conductance. However, several studies suggest that in some epithelia with apical NaCl cotransport, the conductance of the basolateral cell membrane is not large enough to account for the transcellular chloride flux on the basis of electrodiffusion alone [13, 23]. In these epithelia a component of chloride efflux from the cell must be electroneutral.

0022-2631/82/0065-0185 $02.40

The quantitative role of electrodiffusive *vs.* electroneutral chloride transport across the basolateral cell membrane of the *Necturus* proximal tubule is unknown. Therefore, three aspects of chloride transport across the basolateral cell membrane were evaluated in the present study: (i) the total cell membrane conductance and the chloride conductance, (ii) the Cl^- electrochemical driving force, and (iii) the net flux of chloride following basolateral chloride concentration changes. We found that the chloride conductance of the basolateral cell membrane is too low to account for the estimated chloride flux if it were to occur by electrodiffusion alone. Therefore chloride movement across the basolateral cell membrane must include an electrically silent transport mechanism. Part of this research is published elsewhere in abstract form [19].

Materials and Methods

Experimental Approach

The mechanism of Cl^- movement across the basolateral cell membrane of proximal tubule cell of the doubly-perfused *Necturus* kidney was studied in three ways.

First, the total resistances of the apical and basolateral cell membranes and the paracellular shunt were determined from the transepithelial resistance, the cell membrane resistance in parallel, and the resistance ratio of the apical and basolateral membranes. The contribution of Cl^- to the total resistances was assessed by comparing the total resistances in control solutions with values obtained after lowering Cl^-. In addition, the contribution of Cl^- to the cell membrane potential differences and the electromotive forces acting on Cl^- was determined from measurements of transepithelial and basolateral cell membrane potential differences in control and low Cl^- solutions.

Second, the electrochemical driving force for Cl^- movement was obtained from measurements of basolateral membrane potential and intracellular Cl^- activity.

Third, the net flux of chloride was estimated from the change of intracellular Cl^- activity when the basolateral solution was switched from control to a low Cl^- solution.

These techniques were designed to address the following questions: is the Cl^- conductance of the basolateral cell membrane of the *Necturus* proximal tubule large enough to account for the flux of Cl^- through an electrodiffusive pathway or is the movement of Cl^- electroneutral?

Kidney Preparation

Adult specimens of *Necturus maculosus* were obtained from Connecticut Valley Biological Supply Co. (Southampton, Mass.), kept in an aquarium at 15 °C for at least one month prior to use, and fed live goldfish. Animals were anesthetized in 0.67 g/liter tricaine methane sulfonate (Finquel, Ayerst, N.Y.). The kidneys were prepared and doubly perfused via the aorta and portal vein as described previously [17] with either control or low Cl^- solutions (Table 1). Changes of the luminal solution were accomplished by means of a double-barreled pipette (Theta Style I, R and D Optical Systems, Spencerville, Md.) inserted in the glomerulus. One barrel of the pipette contained the control solution to which

Table 1. Concentration of ions in *Necturus* Ringer

mM	Control	Low Cl^-
Na^+	100.5	94.3
K^+	2.5	2.5
Ca^{++}	1.8	8.0
Mg^{++}	1.0	1.0
Cl^-	98.1	8.1
HCO_3^-	10.0	10.0
H_2PO_4	0.5	0.5
SO_4	–	6.2
Gluconate	–	83.8

All solutions contained 2.2 mM glucose, 15 g · liter^{-1} PVP, and 2000 units · liter^{-1} heparin and were bubbled with 99% O_2 – 1% CO_2 to a pH of 7.6. $CaSO_4$ was added to the low Cl^- solution in order to maintain the Ca^{++} activity at control levels.

0.1% Hercules Green Shade #2 (H. Kohnstamm and Co., N.Y.) was added. This was helpful in the identification of the perfused tubule. The other barrel was filled with low Cl^- solution. Changes of peritubular solutions were achieved with the aid of a four-way valve placed close to the site where the caudal vein was cannulated.

Transepithelial and Cell Membrane Potential Differences

Conventional microelectrodes were drawn on a horizontal microelectrode puller (Model PD-5, Narishige Scientific Instruments, Tokyo, Japan) from 1.2 mm OD and 0.6 mm ID, fiber-containing glass capillaries (Federick Haer & Co., Brunswick, Me.) and filled with 1 M KCl. Microelectrodes for transepithelial measurements were beveled to 10 MΩ (Model 1300 Beveler, W.P. Instruments, New Haven, Conn.) in order to minimize impalement damage.

Potential differences were measured by means of an electrometer (Model 725, W.P. Instruments). All microelectrode-electrometer connections were made via Ag/AgCl half cells. Potential differences were measured with reference to a 3-M KCl flowing junction in the Ringer solution above the kidney. The flowing junction was also connected to ground with a Ag/AgCl half cell. Basolateral membrane potential difference, (V_{bl}) and transepithelial potential difference (V_{te}) were measured by means of intracellular and intraluminal impalements with respect to a ground electrode in the bathing solution. The apical potential difference (V_a) was calculated from:

$$V_a = V_{te} - V_{bl}. \tag{1}$$

Measurements of V_{te} and V_{bl} were not carried out in the same tubules; therefore, average values were used to calculate V_a.

Transepithelial Resistance

One current passing and two voltage recording microelectrodes were placed in the lumen of a straight portion of the early proximal tubule. The position of all the electrodes was verified as described previously[1]. Briefly, resistance measurements were performed only if during control perfusion all microelectrodes in the lumen recorded the same transepithelial potential difference. Simi-

[1] Guggino, W.B., Windhager, E.E., Boulpaep, E.L., Giebisch, G. 1981. Cellular and paracellular resistance of the proximal tubule of the *Necturus* kidney. *J. Membrane Biol.* (*submitted*).

larly, measurements were acceptable only when the same reversible hyperpolarization was obtained upon changing the luminal perfusion from the control to a low Cl^- solution and back to control solution. Interelectrode distance was measured with an ocular micrometer.

Current pulses of 2×10^{-7} A and 0.5 sec duration were passed through the most distally located of the three electrodes by means of a constant current source (Channel B Model KS 700, W.P. Instruments). The electrotonic potential difference was recorded simultaneously by the other two microelectrodes by means of two electrometers (Channel A Model KS 700 and Model 725, W.P. Instruments). Electrotonic voltage deflections were measured with reference to a 3-M KCl agar bridge in the Ringer solution above the kidney. The agar bridge was connected to ground with a Ag/AgCl half cell.

The technique for the determination of R_{te} by cable analysis has been described previously [10]. By treating the tubule as a single infinite cable, the length constant (λ_ℓ, μm) of the luminal cable was determined from the inverse of the slope of a log plot of electrotonic potential difference *vs.* distance. The transepithelial specific resistance (R_{te}, $\Omega\,cm^2$) was then estimated from the equation:

$$R_{te} = \frac{2\rho_\ell \lambda_\ell^2}{a} \tag{2}$$

where ρ_ℓ is the luminal fluid volume resistivity (100 $\Omega \cdot$ cm) for *Necturus* Ringer solution) and a, the inner radius.

Cell Membrane Resistance

The parallel resistance (R_z) of apical and basolateral membranes was obtained from the spread of intraepithelial current injection according to the cable analysis technique first used by Windhager et al. [29] in *Necturus* proximal tubule and subsequently by Anagnostopoulos and Velu [5]. A detailed description of this technique has been published previously[2].

Current pulses of 2.5×10^{-8} A were injected through an unbeveled intracellular microelectrode, and the resulting voltage deflections were detected at several points along the tubule by means of a series of sequential cell impalements with microelectrode. The distance between current and measuring microelectrodes was always greater than the tubule diameter and as long as 700 μm.

Assuming that the proximal tubule is a sheet wrapped into an infinite tubule, the voltage attenuation resulting from intraepithelial current injection was described by the following equation.

$$\Delta V_x = \frac{\rho_c \lambda_c I_o}{4\pi a d} e^{-x/\lambda_c} \tag{3}$$

where ΔV_x is the voltage deflection at a distance x from the current source, ρ_c is the cell cable specific resistance ($\Omega \cdot$ cm), I_o is the input current, λ_c the length constant of the cellular cable, a, the inner tubule radius, and d, the thickness of the cell layer. λ_c was determined from the slope of a log plot of ΔV *vs.* distance and ρ_c from the intercept V_o using the equation

$$\rho_c = \frac{4\pi a d V_o}{\lambda_c I_o} \tag{4}$$

R_z is then given by

$$R_z = \frac{\lambda_c^2 \rho_c}{d}. \tag{5}$$

[2] *See* footnote 1, p. 186

Resistance Ratio

The ratio of apical (R_a) to basolateral (R_{bl}) resistance was estimated from the voltage ratio V_a/V_{bl}. Current pulses of 2×10^{-7} A and 0.5 sec duration were injected into the lumen of the tubule with a microelectrode. At another site along the tubule a second microelectrode was inserted sequentially into a cell and then into the lumen of the proximal tubule. The distance between the current and measuring microelectrode was kept constant during the experiment. The resistance ratio was determined from the equation:

$$\alpha = \frac{\Delta V_{te}}{\Delta V_{bl}} - 1 \tag{6}$$

where ΔV_{bl} and ΔV_{te} are the electrotonic potential differences with the electrode in the cell and in the lumen, respectively.

Individual Cell Membrane and Paracellular, Resistances, and Electromotive Forces

According to a simple equivalent circuit model of the proximal tubule [9] which includes all resistances lumped into three components, the apical and basolateral cell membrane resistances and the resistance of the shunt, R_a, R_{bl} and R_s (shunt resistance) were calculated from the following equations:

$$R_{te} = \frac{(R_a + R_{bl}) R_s}{R_a + R_{bl} + R_s} \tag{7}$$

$$R_z = \frac{R_a \cdot R_{bl}}{R_a + R_{bl}} \tag{8}$$

$$\alpha = \frac{R_a}{R_{bl}}. \tag{9}$$

Likewise, the electromotive forces of the apical, E_a, and basolateral, E_{bl}, membranes were calculated from:

$$E_{bl} = V_{bl} + V_{te} \frac{R_{bl}}{R_s} \tag{10}$$

$$E_a = V_a + V_{te} \frac{R_a}{R_s}. \tag{11}$$

In the calculations of electromotive forces the emf of the shunt, E_s, was neglected. This assumption is justified because with symmetrical solutions on both sides of the tubule, E_s is small [11] and therefore would contribute only an insignificant error to the calculation of E_a and E_{bl}.

Intracellular Chloride Activity

Chloride ion specific electrodes were manufactured by means of a modification of the technique of Fujimoto and Kubota [16]. Electrodes were dipped for 3 sec into a 0.1% solution of silicone polymer (1107 fluid, Dow Corning Corp., Midland, Mich.), in acetone, and heated at 300 °C for one-half hour. Electrodes were back-filled with a small quantity of Cl^- specific ion exchanger (Corning #477315).

Cl^- electrodes were gently beveled (Model 1300, Beveler, W.P. Instruments) and viewed under a microscope to assess tip diameter. Usable electrodes were those with tips of diameters of $< 1\mu m$. After beveling, the electrodes were back-filled with 0.5 M KCl. The tips of the Cl^- electrodes were immersed in 100 mM NaCl for several hours before use.

To assess the cellular Cl^- activity in single proximal tubule cells, impalements were made in the same tubule with both chloride specific and 1 M KCl conventional microelectrodes (resistance 30–70 MΩ). The voltages of both the Cl^- specific and the conventional microelectrodes were recorded simultaneously by means of a dual channel very high impedance electrometer (Model F-223A Dual Channel Electrometer, W.P. Instruments). Each experiment represented a single measurement on one tubule.

Cl^- electrodes were calibrated in pure solutions of 5, 10, 50 and 100 mM KCl solutions. The slope (S) of the electrode response was determined from the regression line of voltage *vs.* the log Cl^- activity. Intracellular Cl^- activity was calculated from the following equation:

$$a^i_{Cl} = a^{bl}_{Cl}\, 10^{\frac{(V_{Cl} - V_{bl})}{S}} \tag{12}$$

where a^i_{Cl} and a^{bl}_{Cl} are intracellular and basolateral solution Cl^- activities, respectively, and V_{Cl} the voltage change in the Cl^- electrode from the Ringer's to the cell. The average S of electrodes used in these experiments was −53.4 mV/10-fold change in Cl^- activity. The 95% response time of electrodes was 1 sec (determined from rapid changes of the Cl^- activity of the perfusion solutions).

The selectivity of the Cl^- electrode (k) to gluconate and HCO_3^- was determined from:

$$k_{Cl,A} = 10^{\frac{V_{100A} - V_{100Cl}}{S}} \tag{13}$$

where V_{100A} is the voltage reading of the Cl^- electrode in either 100 mM $NaHCO_3$ or gluconate and V_{100Cl} the voltage in 100 mM KCl. The selectivity of the Cl^- electrodes to HCO_3^- and gluconate were 0.10±0.01 and 0.03±0.01, respectively. Because the activity of HCO_3^- in *Necturus* Ringer solution is about 7 mM, the contribution of HCO_3^- to V_{Cl} is <1 mV. As a result, this error was neglected in our calculation of a^i_{Cl}.

Net Cl^- Flux Across the Basolateral Cell Membrane

A net flux of Cl across the basolateral cell membrane (J_{Cl}) was estimated from the change in a^i_{Cl} when the basolateral solution was switched from control to low Cl^- solution. Impalements were made in the same proximal tubule with a Cl^- sensitive and a conventional microelectrode, and the change in a^i_{Cl} was continuously monitored following a reduction only in a^{bl}_{Cl}. J_{Cl} was estimated from the initial rate of change of a^i_{Cl} from the following equation:

$$J_{Cl} = -\frac{V}{A\gamma}\frac{da^i_{Cl}}{dt} \tag{14}$$

where V is the volume, A the area, and γ the activity coefficient for Cl^-. The cell volume was assumed to be constant throughout the experiment. V/A was estimated to be equal to cell height (h), assuming the cell is a cube and taking A as cm^2 of tubule epithelium. These dimensions are equivalent to those used to determine membrane resistances.

Statistics

Results in this study are reported as mean values ±SE. Student t tests were sued for comparison of means. It was not possible to determine R_a, R_{bl}, R_s, E_a, E_{bl} and V_a on the same tubule. In these instances, the values reported were combinations of means from several experiments.

Table 2. The effects of lowering a_{Cl} on transepithelial and cell membrane potentials and electromotive forces

Apical solution	Control	Low Cl^-	Control
Basolateral Solution	Control	Low Cl	Low Cl^-
V_{bl} (mV)	−62±0.06 (69)	−74±1.6 (24)[a]	−66±1.1 (25)[a]
V_a (mV)	+58	+61	+81
V_{te} (mV)	− 3±0.4 (28)	−12±1.5 (18)[a]	+15±1.1 (23)[a]
E_{bl} (mV)	−84	−105	
E_a (mV)	− 7	−32	

V_{bl}, E_{bl}, and V_{te} were determined with respect to a reference ground electrode in the basolateral solution, V_a and E_a with respect to a reference inside the cell.

[a] $P < 0.01$.

Results

The Effect of Low Extracellular Cl^- on Transepithelial and Cell Membrane Potentials

In order to evaluate the contribution of Cl^- to the transepithelial and cell membrane potentials, both V_{bl} and V_{te} were monitored during rapid changes in extracellular Cl^- activity. The data are summarized in Table 2.

When the activity of Cl^- is lowered from 74 to 6 mM in apical and basolateral solutions simultaneously (Table 2) both V_{bl} and V_{te} hyperpolarize significantly over control values, while V_a is only slightly changed. Similarly, when the activity of Cl^- is lowered asymmetrically, on only the basolateral side, V_{bl} hyperpolarizes; in contrast, under this condition V_{te} becomes positive. The response of V_{bl} and V_{te} to the lowering of basolateral Cl^- activity is relatively rapid, reaching a full response within 2 min of the initial change of Cl^- activity.

The hyperpolarization of V_{bl} when the activity of Cl^- is lowered in both the apical and basolateral solutions or only on the basolateral side is not what would be expected if the basolateral membrane were highly conductive to Cl^-. As described by Hodgkin and Horowicz [20] for muscle fibers, a sudden reduction of a_{Cl} at constant a_{K^+} should cause a transient depolarization of the membrane potential if the basolateral membrane is permeable to Cl^-. The lack of depolarization of V_{bl} in these experiments could result from several mechanisms, which are discussed in detail below.

The depolarization of V_{te} during unilateral lowering of Cl^- on the basolateral side is consistent with a high transepithelial Cl^- conductance. Boulpaep [11] has shown that in view of the high resistance of the

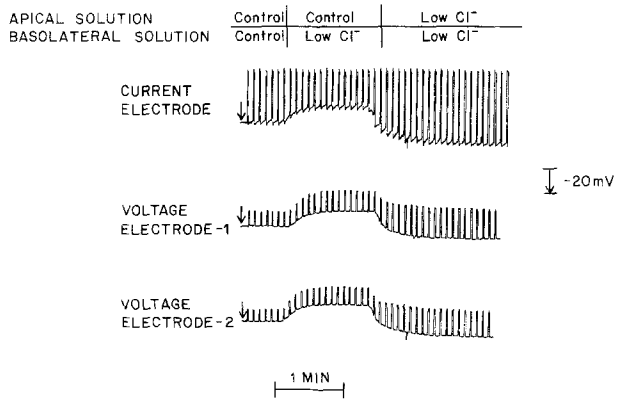

Fig. 1. The three traces represent the transepithelial voltage recordings of three electrodes in the lumen of a *Necturus* proximal tubule. The upper trace is a recording from the current electrode and the lower two traces those of voltage measuring electrodes. The distances between electrodes are 150 and 190 μm, respectively. The arrows mark the time at which all electrodes are recording V_{te} (−5 mV) in control solution prior to current injection. Current pulses appear as spikes superimposed on V_{te}. Electronic voltage deflections recorded by the current electrode are off the scale of the tracing. Perfusing low Cl^- solution on the basolateral side only, depolarizes V_{te} recorded by each electrode. Perfusing low Cl^- solution on both the apical and basolateral sides hyperpolarizes V_{bl} over control values

cell membranes relative to the shunt resistance, changes in V_{te} resulting from diffusion potentials approximate the changes of the electromotive force of the shunt. Therefore the depolarization of V_{te} after basolateral Cl^- reduction results from the induction of a Cl^- concentration difference across the highly Cl^- selective paracellular shunt. It is well known that the Cl^- conductance of the shunt in the *Necturus* proximal tubule exceeds the Na^+ conductance [1, 7, 22].

Measurement of V_{te} in amphibian proximal tubules vary over a considerable range [14]. Because tubule damage could result in an underestimate of V_{te}, in this study microelectrodes used for transepithelial elements were beveled to minimize damage.

Effect of Low Cl^- on Transepithelial Resistance

The total transepithelial resistance of the *Necturus* proximal tubule was determined in control conditions and after the reduction of the Cl^- activity in both apical and basolateral solutions. A typical experiment of transepithelial resistance is illustrated in Fig. 1. Three electrodes were placed in the lumen of a proximal tubule. Because of the difficulty of successfully inserting three microelectrodes in the lumen of a proximal tubule and maintaining them

Table 3. Luminal cable properties of the proximal tubule

	Control	Low Cl
λ_l (μm)	729 ± 67	1377 ± 148[a]
R_{te} (Ω · cm²)	261 ± 58	765 ± 159[a]
a (μm)	57 ± 3	57 ± 3
n	15	15

[a] $P < 0.01$.

properly localized during solution changes, it was necessary to verify the location of the electrodes throughout the experiment. This was accomplished by monitoring V_{te} recorded by the three electrodes throughout the experiment. As shown in Fig. 1, all the electrodes recorded the same control V_{te} and the same changes in V_{te} during low Cl^- perfusion. This indicates that all three electrodes remained in the lumen throughout the experiment.

After verifying the luminal position of the electrodes, current pulses were passed through one electrode and the current spread along the tubule recorded by the two voltage sensing electrodes. As expected, electronic voltage deflections diminish with distance from the current electrode. It is to be noted that following the replacement of the basolateral solution by a low Cl^- solution the transepithelial potential recorded by the electrodes depolarizes. At the same time the superposed voltage pulses increase significantly in magnitude. Similarly, when both apical and basolateral solutions are switched to solutions with a low Cl^- activity the transepithelial potential hyperpolarizes and again the electrotonic deflections increase in magnitude. We concluded from the increase in the magnitude of the transepithelial voltage deflections that the transepithelial resistance increases when Cl^- is removed from the bathing medium.

In experiments in which apical and basolateral membranes were perfused with control solution, the average values of λ_l and R_{te} calculated from each individual tubule are given in Table 3. Values of R_{te} in the present study are consistent with those reported previously for the early proximal tubule of *Necturus* from this laboratory, which range from 70 [10] to 255 Ω · cm² [14]. However, they are less than those of Anagnostopoulos et al. [4] who report values of 420 Ω · cm² for R_{te}. The R_{te} of Anagnostopoulos et al. is in the range of the resistances found across the late proximal tubule of *Necturus* which range from 429 [11] to 641 Ω · cm² [14]. Both λ_l and R_{te} increase significantly above control values when Cl^- activity is reduced in both apical and basolateral perfusion solutions (Table 3).

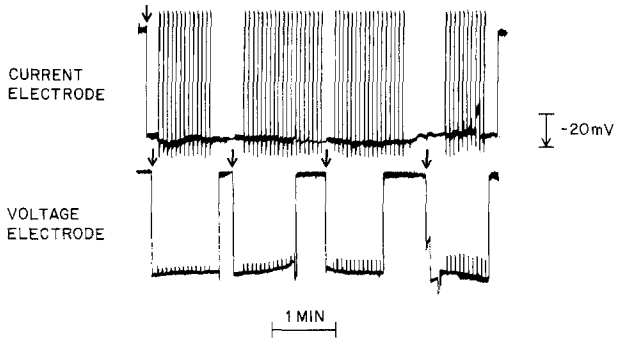

Fig. 2. *The upper trace* represents an intracellular recording of V_{bl} with a current electrode. The arrow marks the point at which the impalement was made across the basolateral cell membrane. While the current electrode remained in the same cell, four intracellular impalements were made with a second electrode at decreasing distance (left to right) from the current electrode, lower trace. The arrows mark the intracellular impalements. During each impalement with the voltage electrode, current pulses were passed through the current electrode. The current pulses appear as spikes superimposed on V_{bl}. The current electrode electronic voltage deflections are off the scale of the tracing

Effects of Low Cl^- on Cell Membrane Resistances in Parallel (R_z) and on the Cell Membrane Resistance Ratio (α)

In order to determine the relative contribution of the cellular resistance to the transepithelial resistance and to quantify the chloride conductance of the cell membranes, both R_z and α were determined in control and low Cl^- solutions.

A typical experiment in which R_z was determined is illustrated in Fig. 2. Four cell impalements were made sequentually along the tubule with a voltage sensing electrode with the current electrode remaining stationary. As expected from Eq. (2), voltage deflections increased exponentially as the measuring electrode was moved closer to the current electrode. The observation that electrode impalements resulted in similar basolateral cell membrane potentials is consistent with the view that the *Necturus* proximal tubule cells are coupled.

The results of 20 experiments are presented in Table 4. In control tubules λ_c in the present study is similar to the values reported for free-flow conditions in *Necturus* by Windhager et al. [29] and by Anagnostopoulos and Velu [5] who both found λ_c to be 200 μm. In addition, Anagnostopoulos and Velu [5] reported a parallel cell membrane resistance of $1786\,\Omega\cdot cm^2$, a value also close to that observed in the present study.

No significant differences in R_z were found when both apical and basolateral sides of the cells were exposed to either control or low Cl^- solutions. Because R_z is comprised solely of cell membrane resistances and does not contain a paracellular component, the observed increase in R_{te} (Table 3) in low Cl^- solution must be limited to a change in R_s.

Table 4. Cell cable resistance properties and resistance ratio

	Control	Low Cl
λ_c (μm)	257± 25	220± 23.5[a]
ρ ($\Omega\cdot cm$)	5837±1139	8480±1895[a]
R_z ($\Omega\cdot cm^2$)	1494± 114	1487± 114[a]
a (μm)	63± 3	56± 3
n	10	10
$R_a/R_{bl}(\alpha)$	2.9±0.3	3.0±0.4
n	10	9

[a] NS.

Recently, Anagnostopoulos et al. [14] have reevaluated the various techniques for estimating R_z by cable analysis. They pointed out that measurements of R_z could be inaccurate because of "cross talk" between luminal and cell cables. This problem arises when current, injected into the cell cable, leaks into the lumen of the tubule. If enough current leaks into the lumen and the λ_c is small, the current in the lumen acts as an additional current source in the cell cable and interferes with the measurement of R_z. However, as pointed out by Anagnostopoulos et al. (*see* Fig. 2 reference 4), the interference of luminal current in the measurement of λ_c is significant only if the current electrode and the voltage electrodes are placed in cells at distances greater than 700 μm, whereas at distances less than 700 μm the error due to luminal current entering the cell cable is too small to be experimentally detectable. It should be noted, however, that at distances exceeding 700 μm, where according to Agnostopoulos et al. the current entering the cell cable from the lumen may become significant, the amplitude of voltage deflections using reasonable current strength becomes too small to be accurately recorded. In our experiments all measurements of cellular electronic voltage deflections were made at distance $\leqq$700 μm from the current source. As shown by Anagnostopoulos et al., such measurements are not subject to significant interference and error from "cross talk" between luminal and cellular current flow.

One way to test directly the reliability of measurements of R_z experimentally is to increase the resistance of the shunt without affecting the resistance of the cell membranes. If there is significant current "cross talk" between cell and luminal cable then changes in R_s and subsequently λ_l should be reflected in λ_c. If there is no significant cross talk then λ_l should be independent of λ_c. In our experiments λ_l increased almost two times from control to

Table 5. Cellular and paracellular resistances

	Control	Low Cl
R_{bl} ($\Omega \cdot cm^2$)	2018	1893
R_a ($\Omega \cdot cm^2$)	5854	5948
R_s ($\Omega \cdot cm^2$)	270	765

low Cl^- perfusion (Table 3) while λ_c did not change significantly. These data suggest that the techniques for measuring R_z in our study are not significantly influenced by cable-to-cable current leaks. We conclude that measurements of R_z by cell cable analysis in our preparation are valid as long as the distances between current and voltage measuring electrodes do not exceed 700 μm.

As shown in Table 5, there are no significant differences in resistance ratio of apical and basolateral cell membranes when the kidney is perfused with control or with low Cl^- solutions in both apical and basolateral fluid compartments. The insensitivity of the cell membrane resistances to reduction in $a_{Cl}^{a,bl}$ is consistent with a low Cl^- conductance of tubular cell membranes.

Effect of Low Cl^- on Individual Resistances and Electromotive Forces

The magnitude of R_a, R_{bl} and R_s was determined from the values of R_{te}, R_z and R_a/R_{bl}. The contribution of Cl^- to these resistances was assessed by lowering Cl^- in both apical and basolateral solutions. The data are summarized in Table 5.

In control perfusions, the shunt resistance of 270 $\Omega \cdot cm^2$ is approximately 30 times less than the total transcellular resistances, $R_a + R_{bl}$ which is 7872 $\Omega \cdot cm^2$. This is consistent with the view that the *Necturus* proximal tubule is a leaky epithelium. Similar values for $R_a + R_{bl}$ were first reported by Windhager et al. [29]. Their data were the first to support the view that a low resistance pathway exists between the cell of the *Necturus* proximal tubule, but the cell membranes have a relatively high transverse resistance. Kimura and Spring [22] have estimated the total resistance of the shunt from the isotopic permeabilities of Cl^- and Na^+ to be 233 $\Omega \cdot cm^2$, a value remarkably similar to ours.

An important finding of the present experiments was that in low Cl^- perfusion R_s increases three times while R_a and R_{bl} are not significantly changed. Assuming a negligible contribution of Cl^- and/or gluconate to the shunt conductance in low Cl^- solution, a minimum transference number (t_s for Cl^-) of the shunt can be calculated from the increase in R_s from control to low Cl^- solutions:

$$t_{s,Cl} = 1 - \frac{R_s^{control}}{R_s^{Low\,Cl}}. \tag{15}$$

The minimum value observed of 0.65 is reasonably close to the estimate of paracellular Cl^- conductance of 0.78 obtained from transepithelial NaCl dilution potential measurements [7] and is almost identical to the chloride transference number of 0.68 obtained from tracer experiments [22]. These data, in addition to the described changes in V_{te} and V_{bl} during lowering of a_{Cl}^{bl}, further support the notion that the shunt is the major conductive pathway for Cl^- movement across the *Necturus* proximal tubule. In sharp contrast, the conductance of the cell membranes to Cl^- is too low to be detected by the methods used in the present study.

In a previous study [9], the transference number of Cl^- of the basolateral cell membrane of the *Necturus* proximal tubule was reported to be 0.3, while in the present study we have found that the Cl^- conductance of the basolateral membrane is low. The difference is that in the earlier study sulfate was used as a replacement ion for Cl^-. Because of the low solubility of $CaSO_4$, replacement of Cl^- by sulfate places a maximum limit on the Ca^{++} activity of the solution.

Using the values of R_a, R_{bl}, and R_s along with V_{bl} and V_{te}, it is possible to evaluate, from Eqs. (10) and (11), the changes in electromotive forces during changes in extracellular chloride. The electromotive forces, E_a and E_{bl} are the potentials that would be observed across the apical and basolateral membranes if there were no current flow through the paracellular shunt. For example, under control conditions (Table 2) the profile of electromotive forces differs from that of the measured membrane potential. The calculated E_{bl} is more negative than V_{bl} and E_a is much more negative than V_a. The differences between measured membrane potentials and electromotive forces result from current flow through the low resistance shunt. The current flow through the shunt in the basolateral to apical direction causes a depolarization of V_{bl} compared to the value of E_{bl} and a reversal in the polarity of E_a compared to V_a.

When the activity of Cl^- is lowered in both apical and basolateral solutions both E_a and E_{bl} hyperpolarizes over control electromotive forces. The hyperpolarization of E_{bl} is not what is predicted if, as the resistance measurements show, the basolateral membrane has a low conductance to Cl^-. E_{bl} should depolarize after a reduction of the activity of Cl^- in both apical and basolateral solutions if the

basolateral cell membrane has an appreciable Cl^- conductance. If the Cl^- conductance of the basolateral cell membrane is low then E_{bl} should remain unchanged during a reduction of Cl activity in both the apical and basolateral solutions.

Effects of SITS and Low HCO_3^- on the Hyperpolarization of V_{bl}

If the hyperpolarization of V_{bl} during a reduction in the Cl^- activity of the basolateral solution is caused by an increase in E_{bl} similar to the hyperpolarization seen during a reduction of a_{Cl} in both apical and basolateral solutions, several mechanisms could be responsible. One explanation is that the basolateral membrane is permeable to gluconate. Given a finite permeability, a gluconate concentration gradient directed from the basolateral fluid to the cytoplasm would hyperpolarize the cell following replacement of extracellular Cl^- by gluconate ions. An alternate explanation is that the basolateral membrane conductance to Cl^- is normally low and that the lowering of a_{Cl}^{bl} affects the permselectivity of the membrane to other ions. For example, the K^+ permselectivity of the basolateral cell membrane of both the *Necturus* proximal tubule [27] and the perfused rabbit proximal tubule [8] is sensitive to changes in basolateral pH. The K^+ permeability is reduced in acid solutions and increased in alkaline solutions. If Cl^- ion undergoes exchange for HCO_3^- in the *Necturus* proximal tubule, then lowering basolateral Cl^- activity and steepening the transmembrane concentration gradient would cause an increased efflux of Cl^- across the basolateral cell membrane (Fig. 5) and a stimulation of HCO_3 uptake into the cells. The resulting increase in intracellular pH would increase P_K and hyperpolarize V_{bl}. It should also be noted that reductions in P_{Na} or P_{HCO_3} or increases in a_K^i or a_{Na}^i would also add to the hyperpolarization of V_{bl}.

In order to test the hypothesis that HCO_3^- is involved in the hyperpolarization of V_{bl} during low Cl^- perfusion, two types of experiments were performed. In the first series of experiments, HCO_3^- was removed from both apical and basolateral control solutions and replaced with 10 mM Hepes, adjusted to pH 7.6, and gassed with 100% O_2. Following the substitution, the perfusion solution on the basolateral side of the proximal tubule cell only was rapidly replaced with low Cl^- solution while keeping the solutions on both sides HCO_3 free (top line, Table 6). In the second series of experiments, the stilbene derivative SITS (4-acetamido-4′-isothiocyanostilbene-2,2′-disulfonic acid), a known inhibitor of anion exchange in red cells, was added at a concentration of 5×10^{-4} M to the control perfusion solution on both sides of the tubule for 15 min. Only the solution on the basolateral side was then rapidly switched to a low Cl^- solution, containing SITS.

Table 6. The effects of HCO_3^- removal and SITS treatment on the hyperpolarization of V_{bl} during basolateral low Cl^- perfusion

Apical solution Basolateral solution	Control Control	Control Low Cl^-
V_{bl} (mV) HCO_3^- free	68 ± 2.2 (12)	64 ± 2.7[a] (12)
V_{bl} (mV) SITS	69 ± 1.0 (16)	64 ± 1.3[a] (16)

SITS (5×10^{-4} M) and HCO_3^--free solutions were applied to both apical and basolateral control and low Cl^- solutions.
[a] $P < 0.01$.

The results of both types of experiments are summarized in Table 6. It can be seen that both removal of HCO_3^- and treatment with SITS inhibits the hyperpolarization of V_{bl} which otherwise follows lowering Cl^- on the basolateral side. These data are consistent with our proposal that an anion exchange process could be present in the basolateral cell membrane. The hyperpolarization during low Cl^- perfusion in the basolateral solution would follow an increase in intracellular HCO_3^- through a SITS inhibitable ion exchange pathway.

Table 6 also shows a small but significant depolarization of V_{bl} during either low Cl^- perfusion plus SITS or in HCO_3-free conditions. In view of the low Cl^- conductance of the basolateral cell membrane, the small depolarization can be explained by the effect of a lumen-positive paracellular E_s on V_{bl} when Cl^- is selectively lowered in the basolateral perfusion solution (Table 2).

Effects of Lowering Cl^- on Intracellular Cl^- Activity

Figure 3 shows typical intracellular impalements in the same proximal tubule with both a conventional KCl and Cl-sensitive microelectrode. Impalements were considered successful if the change in potential was rapid upon entering the cell, the intracellular potential remained stable (within 2 mV) for at least 1 min, and the potential returned to the same baseline when the electrode was removed from the cell. The intracellular Cl^- activity was determined according to Eq. (12) by subtracting V_{bl} from V_{Cl}. This procedure assumed that V_{bl} recorded by the two electrodes is the same. The identity of V_{bl} in several cells along the same tubule was shown in Fig. 2. In those experiments all V_{bl} values recorded in the same tubule were within 2 mV. The average V_{bl} in 51

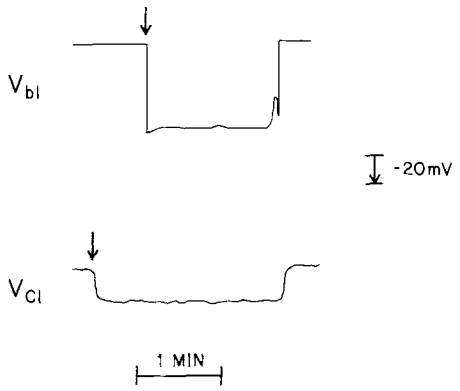

Fig. 3. A typical recording of V_{bl} upper trace and V_{Cl}, lower trace. The arrow marks the point at which the electrode was placed into the cell. Both electrodes were in the same tubule at the same time. Interelectrode distance was always $\leqq 250\,\mu m$

experiments is -66 ± 1 mV and the average a^i_{Cl}, 13.2 ± 0.6 mM.

As has been shown previously [21, 26], Cl^- is above its electrochemical equilibrium in the *Necturus* proximal tubule. In the present experiments, the measured cell Cl^- activity is 13.2 mM, the activity predicted from the membrane potential is 5.4 mM. Figure 4 is a graph of V_{bl} versus $\log a^i_{Cl}$. As is evident from the graph, there is a small but significant correlation ($r = 0.57$, $P < 0.001$) between V_{bl} and a^i_{Cl}. The slope is $+31 \pm 7$ mV per 10-fold change in a^i_{Cl}.

Recently, Shindo and Spring [25] have also reported that there is some degree of correlation between naturally occurring variability of a^i_{Cl} and V_{bl} in the *Necturus* proximal tubule. This correlation exists even though they can detect no change in a^i_{Cl} in a single tubule cell when V_{bl} is varied by transepithelial current flow from a luminally placed axial wire.

In this study we have shown that when a^i_{Cl} is low V_{bl} is high. This correlation is evident whether a^i_{Cl} is low spontaneously in some tubules perfused with control solutions (Fig. 4) or whether a^i_{Cl} is lowered experimentally by perfusing low Cl^- in the basolateral solution (Table 2 and Fig. 5). This apparent correlation of V_{bl} and a^i_{Cl} cannot be simply interpreted as the result of a Cl^- conductance of the basolateral cell membrane. First, as shown in the present study and by Shindo and Spring [25] there is a small Cl^- conductance which would lead to a slope of less than 10% of the ideal slope of 58 mV/10-fold change in intracellular Cl^- activity. Second, the fact that each intracellular Cl^- activity in Fig. 4 is above the equilibrium value predicted from V_{bl} requires additional mechanisms other than a Cl^- conductance to explain the distribution of intracellular Cl^-. What-

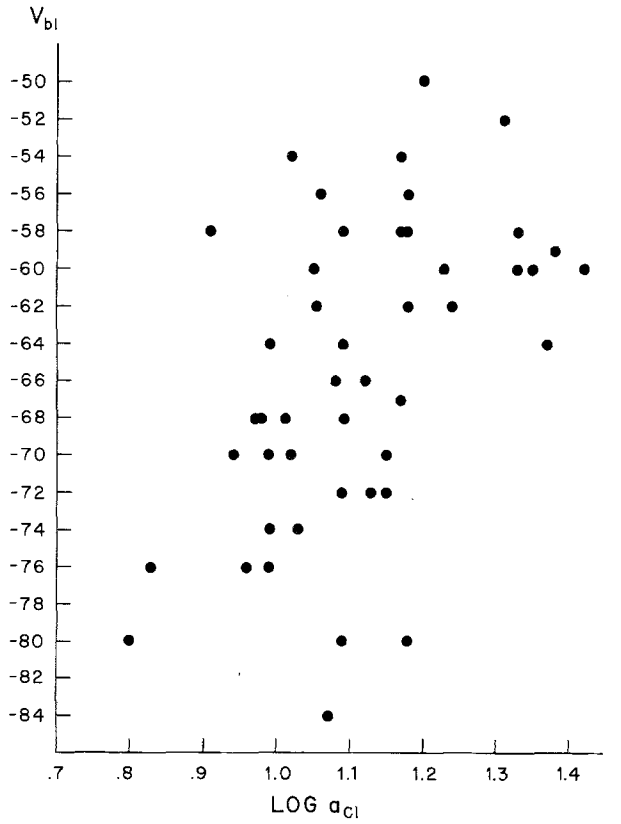

Fig. 4. A plot of 51 measurements of V_{bl} versus $\log a^i_{Cl}$ measured in 51 *Necturus* proximal tubules. The slope of the line is -31 mV/10-fold changes in a^i_{Cl} with a correlation coefficient (r) of 0.57

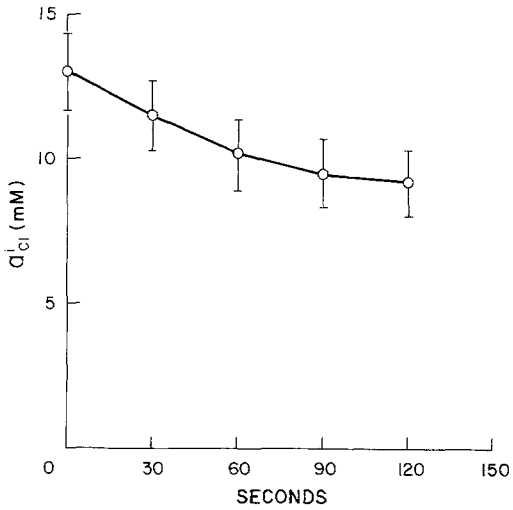

Fig. 5. Represents the average decrease in a^i_{Cl} in six tubules following a switch in the basolateral solution from control to low Cl^-

ever the mechanisms contributing to a higher than equilibrium intracellular Cl^-, it is presently unclear how these mechanisms directly or indirectly affect V_{bl} and a^i_{Cl}.

In order to estimate a net flux of Cl^- across the basolateral cell membrane, a Cl^- sensitive and a conventional electrode were placed in the same tubule and the basolateral solution switched from control to a low Cl^- solution. As illustrated in Fig. 5, a^i_{Cl} falls rapidly from 13.0 ± 1.4 mM [6] in control to 8.6 ± 1.2 mM [6] in low Cl^- solution. The average J_{Cl} for 6 tubules is $1.34 \pm 0.22 \cdot 10^{-10}$ mole $\cdot$ cm$^{-2} \cdot$ sec^{-1}.

It should be noted that the net flux of Cl^- was determined from the initial rate of change in intracellular chloride *vs.* time, following a rapid reduction of basolateral Cl^- only. This approach is likely to result in an underestimate of J_{Cl} for three reasons. (i) The Cl^- activity of the apical solution was kept at control levels when the Cl^- activity of the basolateral solution was lowered. Consequently, the initial rate of change of a^i_{Cl} was probably underestimated due to the possible replenishment of intracellular Cl^- across the apical membrane as a^i_{Cl} falls. (ii) The effect of unstirred fluid layers has to be considered in the doubly perfused, *in vivo* kidney preparation. The effect of an unstirred fluid layer would be to reduce the imposed Cl^- gradient causing an underestimate of the initial rate of change in a^i_{Cl}. (iii) A major assumption in this analysis is that cell volume remains constant despite a reduction of a^i_{Cl}. However, if the cell volume is reduced, the J_{net} will be underestimated.

Discussion

In this study, we have combined measurements of cellular and paracellular resistances, potential differences, electromotive forces, and intracellular Cl^- activities in order to describe the movement of Cl^- across the whole epithelium and across the basolateral membrane of the *Necturus* proximal tubule. The results indicate that the major conductive pathway for Cl^- movement across the *Necturus* proximal tubule is the paracellular shunt and that the conductance of the cell membranes is low.

The fact that the shunt is highly conductive to Cl^- has been well established [1, 7, 22]. In contrast, recent evidence supports the view that the conductance of the basolateral cell membrane to Cl^- is low. Using two completely different techniques from those employed in this study, Shindo and Spring [25] have studied the Cl^- conductance of the basolateral cell membrane of the *Necturus* proximal tubule. In first method, they studied the relative conductance of Cl^- and K^+ by measuring intracellular a^i_{Cl} and $a^i_{K^+}$ as a function of V_{bl}. In their studies the Cl^- permeability of the basolateral membrane was found to be much smaller than the potassium permeability. In the second experiment, current was passed across the epithelium by means of an apical wire to change V_{bl} 20 mV above and 20 mV below the control values, yet no significant change in a^i_{Cl} occurred. Both experiments were interpreted to support the same conclusion, that the Cl^- conductance of the basolateral cell membrane was about 10% of the K^+ conductance of the basolateral membrane [25]. In the present study based on the accuracy of our measurements of membrane resistances, we also conclude that the Cl^- conductance is a fraction of the basolateral cell membrane conductance, which is below our level of detection.

If the basolateral cell membrane has a negligible conductance to Cl^- then lowering Cl^- in both apical and basolateral solutions or in only the basolateral solution should have a very small effect on both the electromotive force, E_{bl}, and the resistance of the basolateral cell membrane, R_{bl}. Reducing Cl^- on the basolateral side only, results in an increase in R_s and E_s produced by a Cl^- gradient across a highly Cl^- conductive paracellular shunt. Whereas, the effects of an increase in R_s would increase V_{bl} and the effects of a positive E_s would tend to depolarize V_{bl}, considering the small value of R_s compared to $R_A + R_{bl}$, a small depolarization of V_{bl} would be expected from the combined changes in E_s and R_s. We found, however, that V_{bl} actually hyperpolarized after basolateral low Cl^- perfusion. This phenomenon was first reported by Anagnostopoulos [2] who showed that V_{bl} hyperpolarized by about 4 mV when basolateral Cl^- activity was lowered by replacement with several organic anions.

Anagnostopoulos and Planelles [3] also found that the hyperpolarization of V_{bl} after basolateral Cl^- replacement could be blocked in HCO_3^--free solutions. We confirmed this observation and showed in addition that the hyperpolarization during Cl^- reduction is inhibited both by HCO_3^- removal at constant pH and by addition of SITS.

There is evidence that the removal of extracellular Cl^- from sheep heart Purkinje fibers results in a hyperpolarization of the membrane potential [28]. In this preparation removal of Cl^- causes an alkalinization of the cell, a decrease in intracellular Cl^- and a hyperpolarization of the cell membrane potential. The process is inhibited by SITS. If a similar mechanism operates in the *Necturus* proximal tubule then lowering of extracellular Cl^- could raise intracellular HCO_3^- and pH, and subsequently change K^+ permeability. Indeed, it has been shown that the K^+ permeability of the basolateral membrane of the *Necturus* proximal tubule is pH sensitive [27], such that it increases in alkalosis and decreases in acidosis.

A discussed above, Cl^- is above equilibrium across the basolateral cell membrane. The driving force in control conditions across the basolateral cell membrane estimated from $V_{bl}-E_{Cl}$ is $-21 \pm 3(51)$ mV. This gradient favors the passive exit of Cl^- from the proximal tubule cell if the Cl^- conductance is sufficient. However, we have shown that the Cl^- conductance of the basolateral cell membrane is low.

In order to evaluate fully the nature of the movement of Cl^- across the basolateral membrane, i.e., whether it crosses the membrane through a conductive or electroneutral pathway, a minimum estimate of J_{Cl} across the basolateral cell membrane was obtained by monitoring the Cl^- efflux in a low Cl^- solution. Under conditions of low basolateral Cl^- activity, the driving force favoring Cl^- extrusion across the basolateral cell membrane increases over control to -86 mV. The Cl^- conductance (G_{Cl}) necessary to account for the efflux of Cl^- via a diffusive pathway can be described by the following.

$$G_{Cl}=\frac{(J_{Cl})(F)}{(V_{bl}-E_{Cl})}. \tag{16}$$

Using J_{Cl} of 1.34×10^{-10} mole $\cdot$ cm$^{-2}\cdot$ sec^{-1}, V_{bl}, -66 mV, and $E_{Cl}+20$ mV the minimum G_{Cl} calculated by this method is 1.6×10^{-4} sec $\cdot$ cm^{-2} or 31% of the total G_{bl} ($R_{bl}=1/G_{bl}$). Since the measured G_{Cl} is much less than 31% of the total G_{bl}, it is clear that the conductance of the basolateral membrane is too low to account for Cl^- movement if it were driven solely by the electrochemical gradient. Interestingly, the measured G_{Cl} is not large enough to account for the movement of Cl^- even though there is a large driving force (-86 mV) favoring efflux after Cl^- is lowered in the basolateral solution. Therefore we conclude that an electroneutral pathway for Cl^- exists in the basolateral cell membrane of the *Necturus* proximal tubule. Since the magnitude of the transcellular net Cl^- transport in control conditions is not known with certainty, the contribution of electroneutral transport to overall transcellular Cl^- transport and volume absorption cannot be quantitated.

It is interesting that an increasing amount of data suggests that in leaky epithelia where Na^+ and Cl^- coupled entry has been identified across the apical membrane, the Cl^- conductance of the basolateral membrane is also low. For example, NaCl entry in the *Necturus* gallbladder epithelium at the apical cell membrane occurs via an electroneutral mechanism, driven by the Na^+ gradient [24]. Reuss [23] has shown that G_{Cl} of the basolateral cell membrane of the *Necturus* gallbladder is quite low such that only a small fraction of the Cl^- flux across the basolateral could occur by electrodiffusion. Duffy et al. [13] also suggested a similar mechanism to be operative in the rabbit gallbladder across the serosal cell membrane, a preparation in which Cl^- entry into the cell across the apical cell membrane had been shown to be coupled to Na^+. Apparently, the proximal epithelium of *Necturus* shares with some leaky epithelia the ability to regulate intracellular Cl^- above equlibrium via electroneutral pathways across both apical and basolateral membranes.

The authors wish to thank Mr. Fred Banti for his technical assistance and Dr. S. Lewis for his comments on the manuscript. Dr. W.B. Guggino was supported by a fellowship from the National Kidney Foundation. The study was supported by U.S. Public Health Service Grant #AM-17433.

References

1. Anagnostopoulos, T. 1973. Biionic potentials in the proximal tubule of *Necturus* kidney. *J. Physiol. (London)* **233**:375-394
2. Anagnostopoulos, T. 1977. Electrophysiological study of the antiluminal membrane in the proximal tubule of *Necturus:* Effect of inorganic anions and SCN. *J. Physiol. (London)* **267**:89-111
3. Anagnostopoulos, T., Planelles, G. 1979. Organic anion permeation at the proximal tubule of *Necturus*. An electrophysiological study of the peritubular membrane. *Pfluegers Arch.* **381**:231-239
4. Anagnostopoulos, T., Teulon, J., Edelman, A. 1980. Conductive properties of the proximal tubule in *Necturus* kidney. *J. Gen. Physiol.* **75**:553-587
5. Anagnostopoulos, T., Velu, E. 1974. Electrical resistance of cell membranes in *Necturus* kidney. *Pfluegers Arch.* **346**:327-339
6. Armstrong, W.M., Wojtkowski, W., Bixenman, W.R. 1977. A new solid state microelectrode for measuring intracellular chloride activities. *Biochim. Biophys. Acta* **465**:165-170
7. Asterita, M.F., Boulpaep, E.L. 1975. Ion selectivity of the paracellular pathway in *Necturus* proximal tubule. (*Abstr.*) *Biophys. J.* **15**:228*a*
8. Biagi, B., Sohtell, M., Giebisch, G. 1980. Effects of bath potassium and pH on intracellular potassium activity in rabbit proximal straight tubule. 13th Annual Meeting of the American Society of Nephrology. Washington, D.C. p. 125*A*
9. Boulpaep, E.L. 1967. Ion permeability of the peritubular and luminal membrane of the renal tubular cell. *In:* Transport and Funktion Intracellulärer Elektrolyte. F. Krück, editor. pp. 98-107. Urban and Schwarzenberg, Berlin
10. Boulpaep, E.L. 1972. Permeability changes of the proximal tubule of *Necturus* during saline loading. *Am. J. Physiol.* **222**:517-531
11. Boulpaep, E.L. 1976. Electrical phenomena in the nephron. *Kidney Int.* **9**:88-102
12. Duffey, M.E., Thompson, S.M., Frizzell, R.A., Schultz, S.G. 1979. Intracellular chloride activities and active chloride absorption in the intestinal epithelium of the winter flounder. *J. Membrane Biol.* **50**:331-341

13. Duffey, M.E., Turnheim, K., Frizzell, R.A., Schultz, S.G. 1978. Intracellular chloride activities in rabbit gallbladder: Direct evidence for the role of the sodium-gradient in energizing "uphill" chloride transport. *J. Membrane Biol.* **42**:229–245
14. Forster, J., Steels, P.S., Boulpaep, E.L. 1980. Organic substrate effects on and heterogeneity of *Necturus* proximal tubule function. *Kidney Int.* **17**:479–490
15. Frizzell, R.A., Field, M., Schultz, S.G. 1979. Sodium-coupled chloride ion transport by epithelial tissues. *Am. J. Physiol.* **236** (*Renal Fluid Electrolyte Physiol.* **5**) *F*1–*F*8
16. Fujimoto, M., Kubota, T. 1976. Physiochemical properties of a liquid ion exchanger microelectrode and its application to biological fluids. *Jpn. J. Physiol.* **26**:631–650
17. Giebisch, G. 1961. Measurements of electrical potential differences on single nephrons of the perfused *Necturus* kidney. *J. Gen. Physiol.* **44**:659–678
18. Grandchamp, A., Boulpaep, E.L. 1974. Pressure control of sodium reabsorption and intercellular backflux across proximal kidney tubule. *J. Clin. Invest.* **54**:69–82
19. Guggino, W.B., Boulpaep, E.L., Giebisch, G. 1980. Electrical properties of proximal tubule cells of the *in vivo* perfused *Necturus* kidney: Chloride reabsorption. (*Abstr.*) *Fed. Proc.* **39**:1080
20. Hodgkin, A.L., Horowicz, P. 1959. The influence of potassium and chloride ions on the membrane potential of single muscle fibers. *J. Physiol.* (*London*) **148**:127–160
21. Khuri, R.N., Agulian, S.K. 1975. Electrochemical potentials of chloride in proximal renal tubule of *Necturus maculosus*. *Comp. Biochem. Physiol.* **50A**:695–700
22. Kimura, G., Spring, K.R. 1978. Transcellular and paracellular tracer chloride fluxes in *Necturus* proximal tubule. *Am. J. Physiol.* **235** (*Renal Fluid Electrolyte Physiol.* **4**):*F*617–*F*625
23. Reuss, L. 1979. Electrical properties of the cellular transepithelial pathway in *Necturus* gallbladder: III. Ionic permeability of the basolateral cell membrane. *J. Membrane Biol.* **47**:239–259
24. Reuss, L., Grady, T.P. 1979. Effects of external sodium and cell membrane potential on intracellular chloride activity in gallbladder epithelium. *J. Membrane Biol.* **51**:15–31
25. Shindo, T., Spring, K.R. 1981. Chloride movement across the basolateral membrane of proximal tubule cells. *J. Membrane Biol.* **58**:35–42
26. Spring, K.R., Kimura, G. 1978. Chloride reabsorption by renal proximal tubules of *Necturus*. *J. Membrane Biol.* **38**:233–254
27. Steels, P.S., Boulpaep, E.L. 1976. Effect of pH on ionic conductances of the proximal tubule epithelium of *Necturus* and the role of buffer permeability. (*Abstr.*). *Fed. Proc.* **35**:465
28. Vaughn-Jones, R.D. 1979. Regulation of chloride in quiescent sheepheart Purkinje fibers studies using intracellular chloride and pH-sensitive micro-electrodes. *J. Physiol.* (*London*) **295**:111–137
29. Windhager, E.E., Boulpaep, E.L., Giebisch, G. 1966. Electrophysiological studies on single nephrons. *Proc. 3rd Int. Congr. Nephrol.* **1**:35–47

Received 23 September 1981